Efficient impurity-bath trial states from superposed Slater determinants

Izak Snyman, Serge Florens

Efficient impurity-bath trial states from superposed Slater determinants

Izak Snyman
Mandelstam Institute for Theoretical Physics, School of Physics, University of the Witwatersrand, Braamfontein 2000, Johannesburg, South Africa

Serge Florens
Institut Néel, CNRS and Université Grenoble Alpes, F-38042 Grenoble, France

(Received 2 July 2021; revised 8 November 2021; accepted 9 November 2021; published 19 November 2021)

The representation of ground states of fermionic quantum impurity problems as superpositions of Gaussian states has recently been given a rigorous mathematical foundation [S. Bravyi and D. Gosset, Commun. Math. Phys. **356**, 451 (2017)]. It is natural to ask how many parameters are required for an efficient variational scheme based on this representation. An upper bound is $O(N^2)$, where N is the system size, which corresponds to the number parameters needed to specify an arbitrary Gaussian state. We provide an alternative representation, with more favorable scaling, only requiring $O(N)$ parameters, that we illustrate for the interacting resonant-level model. We achieve the reduction by associating mean-field-like parent Hamiltonians with the individual terms in the superposition, using physical insight to retain only the most relevant channels in each parent Hamiltonian. We benchmark our variational ansatz against the numerical renormalization group, and compare our results to other variational schemes of a similar nature to ours. Apart from the ground-state energy, we also study the spectrum of the covariance matrix—a very stringent measure of accuracy. Our approach outperforms some existing variational schemes and remains quantitatively accurate in the numerically challenging near-critical regime.

DOI: 10.1103/PhysRevB.104.195136

I. INTRODUCTION

A. Motivation

The brute force diagonalization of a generic quantum many-body problem requires computational resources that grow exponentially with the system size, and is therefore impracticable for systems with more than a handful of particles. A major achievement in the field of strongly correlated electrons has been the development of numerical methods for special classes of problems that circumvent this exponential barrier. Examples include the numerical renormalization group (NRG) [1] for quantum impurity problems, the density matrix renormalization group (DMRG) [2,3] for one-dimensional lattice problems, and quantum Monte Carlo simulations [4] in situations where the sign problem is manageable. However, these numerical methods typically do not give direct access to useful expressions for correlated ground states in terms of the bare degrees of freedom appearing in the microscopic Hamiltonian. Instead, the ground-state structure must be inferred from the sometimes limited set of observables the method allows one to calculate.

It is therefore desirable to develop methods that provide intuition for the nature of correlated ground states, even in cases where existing methods provide numerically exact answers [5]. A well-established approach in this context revolves around parent Hamiltonians [6]. The idea is to identify a Hamiltonian whose ground state can be computed easily and can serve as an idealization of the correlated state of interest. Since operators do not have to be close to each other to have similar behavior in a restricted subspace, the parent Hamiltonian may be very different from the microscopic one, thus providing a useful perspective on the ground state in question.

An almost trivial example of the parent Hamiltonian idea is Hartree-Fock mean field theory, in which an interacting Hamiltonian is replaced by an optimal noninteracting approximation. Mean-field theory often serves to identify the types of behavior that a system may host. However, there are well-known examples where mean-field theory severely overestimates the ground-state energy or predicts spontaneous symmetry breaking when the true ground state is symmetric. This is typically the case for quantum impurities where even local perturbations can hybridize distinct symmetry broken states. Furthermore, mean-field parent Hamiltonians cannot produce the non-Gaussian correlation functions that often characterize interacting problems. Going beyond noninteracting parent Hamiltonians requires ingenuity and a case-by-case approach. This explains why important classes of many-body problems have to date not benefited from the parent Hamiltonian method.

In this paper, we focus on one such class, namely, quantum impurity models. In this context, a favored method involves constructing variational trial states by forming linear combinations of Gaussian states. Approximations with linear combinations of two Gaussians were already used long ago to obtain a qualitative physical description [7–9]. Adding more terms in the superposition offers a viable route to arbitrary accuracy, as was demonstrated systematically for the spin-boson

model [10,11] and the scaling limit of the anisotropic Kondo Hamiltonian [12]. Recently, Bravyi and Gosset proved analytically that the ground state of an arbitrary fermionic quantum impurity problem can be approximated as a superposition of M Gaussian states, using computational resources that scale cubically in system size and quasipolynomially in the inverse of the accuracy [13]. One motivation for further refinement of such ground-state methods is as follows. It is a challenge to achieve good real-space resolution of correlations for systems with $O(10^3)$ lattice sites. This explains why accurate calculations of the full Kondo screening cloud were only reported in recent years [14,15]. Interesting problems, such as studying the interplay between Kondo correlations and moderate to strong disorder, even in one dimension, are probably beyond the capabilities of established methods such as NRG or DMRG. A fast method that can calculate ground-state correlations for an impurity coupled to real space lattices of at least $O(10^3)$ sites is required. Bravyi and Gosset's results on the computational complexity of quantum impurity problems suggest that methods based on superpositions of Gaussian states could fit the bill. Practical algorithms involve minimizing the expectation value of the energy over the weights of the terms in the superposition and over the parameters of the Gaussian states. Recently, an efficient optimization method has been used [16] to investigate spatial correlations in the notoriously difficult two-channel Kondo problem. This and other existing methods consider each Gaussian state to be completely arbitrary, which means that the number of variational parameters per Gaussian state scales quadratically with the system size. It seems likely that physical insight into the specific system under consideration could be exploited to reduce the number of parameters per Gaussian state. Given the complexity of finding the absolute minimum in a large-scale nonconvex optimization problem, such a reduction, if possible, could prove invaluable.

B. Superposed Gaussians from restricted parent Hamiltonians

In this paper, we demonstrate a strategy to significantly reduce the number of variational parameters per state in Gaussian superpositions. We do so by parametrizing the Gaussian states using noninteracting parent Hamiltonians. This makes the physical meaning of the parameters transparent and allows us to use significantly fewer variational parameters than are required to specify an arbitrary Gaussian state. We demonstrate our ideas by studying the Interacting Resonant Level Model (IRLM) [17], the simplest quantum impurity problem in which an electronic impurity orbital interacts with a conduction band to produce Kondo correlations. In the past, the IRLM has provided an interesting test bed for studying equilibrium [18–21] and dynamical [22–32] features of impurity models. Our key insight is the following. When an electronic impurity interacts with a conduction band, there are two obvious channels involved. The first is the Hartree channel, where the charge or spin density on the impurity induces a site-dependent inhomogenous charge or spin density in the conduction band. The second is the Fock channel, which leads to a hybridization of the impurity and the conduction band orbitals. We take only these two channels into account when constructing parent Hamiltonians. As a result, the number of variational parameters in our approach only scales linearly with the system size, as opposed to quadratically. We nonetheless obtain results that are significantly more accurate than some competing variational approaches. We also show that pairing-type correlations [33,34] do not play a major role for the model under consideration, so the variational state can be constructed from Slater determinants rather than more general Gaussians that host BCS correlations.

In addition, we emphasize here general symmetry considerations. This provides an alternative perspective on the use of superpositions of a few well-chosen Slater determinants as variational trial states. An important ingredient of quantum impurity models is particle-hole symmetry. While it is only obeyed for a fine-tuned electrostatic potential on the impurity, particle-hole symmetry-breaking terms become irrelevant at Kondo correlated fixed points. If we attempt to approximate the ground state of a fermionic quantum impurity problem by a single Slater determinant $|F\rangle$, the generic structure of $|F\rangle$ will be a Fermi sea in which plane-wave orbitals are replaced by scattering states in the presence of a static impurity. Very often, $|F\rangle$ will break a symmetry that the interacting Hamiltonian H preserves. For simplicity, let us consider a $\mathbb{Z}_2$ symmetry such as the above-mentioned particle-hole conjugation and take its unitary and Hermitian generator to be P. Then $PHP = H$, but $P|F\rangle \neq |F\rangle$. If the true ground state preserves the symmetry, one may conjecture a ground-state approximation of the form $|\psi\rangle = |F\rangle \pm P|F\rangle$, which we call a Slater pair, where the two states in the superposition are related to each other by particle-hole conjugation. Note here that the single-particle orbitals that are naturally associated with $P|F\rangle$ are different from, but not orthogonal to, those associated with $|F\rangle$. It therefore typically requires an enormous number of Slater determinants to express $P|F\rangle$ in the basis associated with $|F\rangle$ and, as a result, $|\psi\rangle$ can potentially describe strong correlations. There is, however, the following pitfall. Since $|F\rangle$ and $P|F\rangle$ are associated with different static scatterers, the orthogonality catastrophe generically causes the overlap $\langle F|HP|F\rangle$ to scale like $N^{-\alpha}$, where N is the number of particles in the system and $\alpha \geqslant 0$ is determined by the phase shifts at the Fermi energy induced by the static scatterers associated with $|F\rangle$ and $P|F\rangle$ [35]. Generically then, $\langle F|HP|F\rangle$ tends to zero in the thermodynamic limit. If this happens, $|\psi\rangle = |F\rangle \pm P|F\rangle$ is no better an approximation to the true ground state than $|F\rangle$ alone. However, the orthogonality catastrophe can be avoided by fine-tuning the scattering phase shifts to produce $\alpha = 0$. A natural way to do this is to associate a noninteracting parent Hamiltonian H_F with $|F\rangle$, that has a similar form to the mean-field Hamiltonian. However, instead of determining the fields that are responsible for static scattering by applying the mean-field self-consistency condition, one views these fields as variational parameters chosen to optimize $\langle\psi|H|\psi\rangle/\langle\psi|\psi\rangle$ for $|\psi\rangle = |F\rangle \pm P|F\rangle$.

The same symmetry considerations were formulated early on within an approximate variational treatment of the spin-boson model [36], known as the Silbey-Harris ansatz [9,37]. The spin-boson model describes dissipation in a quantum mechanical two-level system coupled to a bath of harmonic oscillators. After nonuniversal ultraviolet modes are eliminated from the spin-boson model and the IRLM, the models can be mapped onto each other [38–40]. At weak dissipation,

an ansatz of the form $|\phi\rangle = |+\rangle|B_+\rangle - |-\rangle|B_-\rangle$ accurately approximates the ground state of the spin-boson model. Here $|\pm\rangle$ refers to the state of the two-level system and $|B_\pm\rangle$ describes a bath state in which each oscillator is in the ground state corresponding to an equilibrium position that is shifted, with the shifts depending on oscillator frequency and on the state of the two level system. It has subsequently been shown that the Silbey-Harris ansatz can be systematically improved to arbitrary accuracy by forming a linear combinations of coherent states of the form $|\phi\rangle$ where the oscillator displacements and weights are treated as variational parameters [10,11]. A natural generalization in the fermionic context results in an ansatz:

$$|\Psi\rangle = \sum_{J=1}^{M} f_J(|F_J\rangle \pm P|F_J\rangle). \tag{1}$$

The above variational state is a linear superposition of individual Slater pairs $|F_J\rangle \pm P|F_J\rangle$. In this way, a single ground state is associated with two or more noninteracting parent Hamiltonians $(H_{F,J}, PH_{F,J}P)$. It is important to stress that the argument that we presented here is heuristic. Despite the equivalence between the spin-boson model and the IRLM, the ansatz Eq. (1) is not exactly equivalent to the ansatz employed previously for the spin-boson model [10,11]. Because a Slater pair describes all-fermionic microscopic degrees of freedom (including the impurity), we can use Slater determinants $|F_J\rangle$ in which the impurity and conduction band are hybridized. In the spin-boson model, the microscopic degree of freedom associated with the impurity is a spin 1/2, while those of the bath are bosons, and one cannot construct Gaussian states that hybridize them. Due to the presence of a hybridization channel in the IRLM, we may expect faster convergence with respect to the number M of Slater pairs than was found for the sum of Silbey-Harris terms in the spin-boson model. Indeed, below we find excellent agreement with numerically exact IRLM results, in the challenging regime of strong correlations, for $M = 2$. In contrast, it is not uncommon to employ $M = 8$ to reach good convergence in the same regime of the spin-boson model [10,11].

To assess the accuracy of our trial ground states, we compare to numerically exact results obtained using NRG. Our model possesses an emergent energy scale, the Kondo temperature, that vanishes at the quantum phase transition. As a result, a variational trial state can give a seemingly reasonable approximation to the ground-state energy yet miss important features of the true ground state at the Kondo scale. We therefore need to identify observable quantities that are sensitive to the nontrivial correlations hosted by the IRLM. For this purpose, we demonstrate the utility of the covariance matrix [41,42] Q (also sometimes called the correlation matrix) and, more particularly, its eigenvalues. The covariance matrix can be defined as follows. Imagine viewing a fermionic wave function as a state of a system of N distinguishable particles that just happens to be antisymmetric under particle exchange. The covariance matrix is then N times the reduced density matrix of one of the N particles. All its eigenvalues lie in the interval [0,1]. Owing to the unavoidable entanglement between the hypothetical distinguishable particles that is implied by antisymmetrization, Q never describes a pure state. If (and only if) the fermionic wave function is a pure Slater determinant, Q has N eigenvalues equal to one and all others are zero. The eigenvalues of $Q(1-Q)$ are therefore nonzero only when nontrivial many-body correlations are present. For a generic fermionic impurity problem, there is exponential decay to full occupancy or vacancy, leaving only a handful of eigenvalues significantly different from zero or one. The remaining orbitals, being exponentially close to filled or empty, do not take part in correlations. Once the handful of correlated orbitals are known, an accurate approximation to the ground state can be constructed by solving a few-body problem in the Fock-space built from only these orbitals. The size of this few-body problem is independent of N, the actual system size. It is purely determined by the desired accuracy and the exponential decay rate of the spectrum of Q [13,42]. As a result, the Q matrix contains nearly complete (up to exponentially small errors, that may take nonpolynomial time in N to correct) information about the ground state of a generic fermionic impurity problem. To accurately reproduce the eigenvalues of $Q(1-Q)$ that are significantly different from zero (and the associated eigenvectors) requires that an approximate state accurately captures the many-body correlations of the true ground state. In contrast to this, Hartree-Fock mean field theory approximates all eigenvalues of $Q(1-Q)$ as zero.

The rest of this paper is structured as follows. In Sec. II, we formulate the model that we study and present the discretized version used for numerics. We then provide the explicit form of our ansatz and the associated parent Hamiltonians. At this point, we also discuss the relation between our approach and existing ones. In Sec. III, we present numerical results. We benchmark our ansatz against numerically exact results obtained using NRG and compare to some existing variational approaches for fermionic impurity problems. Having established the reliability of our method, we also present results in a regime inaccessible to NRG. In Sec. IV, we summarize our approach and main conclusions, and provide an outlook on future work. Four appendices contain technical details about our calculations.

II. SYSTEM AND GROUND STATE ANSATZ

A. Model and basic properties

The IRLM describes spinless fermions in a crystal band with edges at $-t$ and t, interacting with a localized orbital. We denote the annihilation operator of the localized orbital by c_{-1}. Band orbitals are labeled by their energy, and the associated annihilation operators are denoted a_ε. We assume a constant density of states in the band. The model incorporates tunneling between the localized orbital and a single site (labeled 0) of the crystal, and a density-density interaction between the localized orbital and crystal site zero. Tunnelling is controlled by the hybridization strength γ and interactions by the coupling constant U. The Hamiltonian reads

$$H_{\mathrm{IRML}} = \int_{-t}^{t} d\varepsilon\, \varepsilon a_\varepsilon^\dagger a_\varepsilon + U\left(n_{-1} - \frac{1}{2}\right)\left(n_0 - \frac{1}{2}\right) + \frac{\gamma}{2\sqrt{t}}\int_{-t}^{t} d\varepsilon\, (c_{-1}^\dagger a_\varepsilon + a_\varepsilon^\dagger c_{-1}), \tag{2}$$

where $n_{-1} = c_{-1}^\dagger c_{-1}$ and $n_0 = c_0^\dagger c_0$ with

$$c_0 = \frac{1}{\sqrt{2t}} \int_{-t}^{t} d\varepsilon\, a_\varepsilon. \tag{3}$$

Throughout this paper, we study the most interesting case, where the Fermi energy is aligned with the on-site energy ($= 0$) of the localized level, so the system possesses particle-hole symmetry. The system then hosts a quantum phase transition. For γ sufficiently smaller than t, the transition occurs at $U_c \simeq -1.3\,t$. For $U > U_c$, the system is in the symmetric phase, with a unique ground state satisfying the expectation value $\langle n_{-1}\rangle = 1/2$. For $U < U_c$, there are two degenerate ground states. The phase transition is associated with spontaneous particle-hole symmetry breaking, and can be diagnosed by applying an infinitesimal on-site energy bn_{-1} to the localized orbital. In the symmetric phase, this produces only an infinitesimal change to $\langle n_{-1}\rangle$. In the broken symmetry phase, on the other hand, $\langle n_{-1}\rangle$ differs from $1/2$ by a finite amount, even for infinitesimal b. Typical of quantum phase transitions, there is also an emergent energy scale in the symmetric phase that vanishes as the critical point is approached. It is associated with the polarizability of the localized orbital and can be defined as

$$T_{\rm K} = \frac{1}{4\chi}, \quad \chi = \partial_b \langle n_{-1}\rangle|_{b=0}. \tag{4}$$

As mentioned earlier, the IRLM can be mapped onto the Kondo model and T_K is nothing but the Kondo temperature [43].

For numerical work, we have to truncate the above thermodynamic system to a finite set of electronic modes. Because we want to make a direct comparison to NRG results and because we want to access long wavelengths at the lowest possible numerical cost, we will employ a logarithmic energy discretization,

$$\varepsilon_{n,\pm} = \pm\frac{1+\Lambda}{2\Lambda}\Lambda^{-n}t \text{ for } n = 0, 1, 2, \ldots, \Omega, \tag{5}$$

with a discretization parameter $\Lambda > 1$. The thermodynamic limit is recovered by sending $\Omega \to \infty$ followed by $\Lambda \to 1$. While NRG becomes numerically too demanding for Λ significantly less than 1.5, it turns out that many quantities reach values close to the thermodynamic limit for Λ between 1.5 and 2. After the logarithmic discretization of the energy, a standard tridiagonalization procedure maps the model onto a Wilson chain [1] with Hamiltonian

$$H = U\left(n_{-1} - \frac{1}{2}\right)\left(n_0 - \frac{1}{2}\right) + \gamma\left(c_{-1}^\dagger c_0 + c_0^\dagger c_{-1}\right) + \sum_{n=0}^{2\Omega-1} t_n (c_n^\dagger c_{n+1} + c_{n+1}^\dagger c_n). \tag{6}$$

Here, the operators c_n with $n \geqslant 1$ are not associated with sites of the physical lattice, but rather with energy shells corresponding to energy scales $\sim t\Lambda^{-n/2}$ above and below the Fermi energy. Hopping between energy shells is controlled by an exponentially decaying hopping amplitude:

$$t_n = \frac{(1+\Lambda^{-1})(1-\Lambda^{-n-1})}{2\sqrt{1-\Lambda^{-2n-1}}\sqrt{1-\Lambda^{-2n-3}}}\Lambda^{-n/2}t. \tag{7}$$

By truncating the chain to 2Ω shells, one imposes an infrared cutoff of $\Lambda^{-\Omega}t$. All the results we present are for the Hamiltonian Eq. (6).

Apart from computing the ground-state energy of the model, we will study the covariance matrix,

$$[Q]_{m,n} = \langle c_m^\dagger c_n\rangle;\ m,\ n \in \{-1, 0, \ldots, 2\Omega\}, \tag{8}$$

where the expectation value is with respect to the ground state. The properties of Q that were cited in the Introduction can be derived by considering the expectation value of an arbitrary additive single-particle operator,

$$\hat{Z} = \sum_{m,n=-1}^{2\Omega} Z_{mn} c_m^\dagger c_n, \tag{9}$$

with respect to the N-particle ground state. On the one hand, $\langle\hat{Z}\rangle = \mathrm{Tr}(ZQ)$. On the other hand, $\langle\hat{Z}\rangle = N\mathrm{Tr}(Z\rho_1)$, where ρ_1 is the reduced density matrix obtained by tracing out all but one particle. Since Z is arbitrary, $Q = N\rho_1$.

The IRLM Wilson chain manifests particle-hole symmetry $H = PHP^\dagger$, where P is the unitary and Hermitian particle-hole conjugation operator,

$$P = \prod_{n=0}^{\Omega}(c_{2n}^\dagger + c_{2n})(c_{2n-1}^\dagger - c_{2n-1}), \tag{10}$$

with action

$$Pc_nP = (-1)^n c_n^\dagger,$$
$$P|0\rangle = c_{2\Omega}^\dagger \ldots c_{-1}^\dagger|0\rangle. \tag{11}$$

B. Slater pair ansatz

The approach outlined in the Introduction then leads to a variational ground-state ansatz of the form

$$|\psi\rangle = \sum_{J=1}^{M} f_J(|F_J\rangle + \sigma P|F_J\rangle), \tag{12}$$

where $\sigma = \pm 1$ is the eigenvalue of $|\psi\rangle$ with respect to particle-hole conjugation P. Here $|F_J\rangle$ is the Slater determinant ground state in the half-filled sector of the parent Hamiltonian

$$H_J = \sum_{n=-1}^{2\Omega} \frac{\varepsilon_n^{(J)}}{\Lambda^{-n/2}} c_n^\dagger c_n + \sum_{n=0}^{2\Omega} \frac{g_n^{(J)}}{\Lambda^{-n/2}}(c_{-1}^\dagger c_n + c_n^\dagger c_{-1}) + \sum_{n=0}^{2\Omega-1} t_n (c_n^\dagger c_{n+1} + c_{n+1}^\dagger c_n). \tag{13}$$

For our definition of P, the ground-state sector (of the symmetric phase) has $\sigma = -1$. The coefficients f_J, and the parameters $\varepsilon_n^{(J)}$ and $g_n^{(J)}$ are determined by minimizing

$$E_{\rm var} = \frac{\langle\psi|H|\psi\rangle}{\langle\psi|\psi\rangle}. \tag{14}$$

In our definition of H_J, we multiply $\varepsilon_n^{(J)}$ and $g_n^{(J)}$ by scaling factors $\Lambda^{n/2}$ appropriate for shell n. This produces a parameter space in which the region that needs to be searched has roughly the same size in every direction. Technical details

of the variational calculation can be found in Appendices A and B.

The parent Hamiltonians H_J are generalizations of the Hartree-Fock mean-field Hamiltonian associated with the model. In the standard mean-field approach, only three effective parameters appear, namely, the two renormalized potentials $\epsilon_{-1}c^\dagger_{-1}c_{-1}$ and $\epsilon_0 c^\dagger_0 c_0$ on the impurity and on-site zero of the chain, respectively, and the renormalized hybridization $g_0(c^\dagger_{-1}c_0 + c^\dagger_0 c_{-1})$ between the impurity and site zero. Indeed, minimizing the energy with respect to a single determinant, one finds a minimum when ε_n and g_n are zero for $n \geqslant 1$, and the remaining parameters obey the expected Hartree-Fock self-consistency conditions:

$$\frac{\varepsilon_{-1}}{\sqrt{\Lambda}} = U\left(\langle n_0\rangle - \frac{1}{2}\right), \tag{15}$$

$$\varepsilon_0 = U\left(\langle n_{-1}\rangle - \frac{1}{2}\right), \tag{16}$$

$$g_0 = \gamma - U\langle c^\dagger_{-1}c_0\rangle. \tag{17}$$

This mean-field ansatz misses crucial Kondo physics. Yet, building a Slater pair ansatz parametrized only with the three mean-field parameters ε_{-1}, ε_0, and g_0 does not lower the energy. Indeed, in the symmetric case where $\varepsilon_{-1} = \varepsilon_0 = 0$, the two members of the pair are equivalent, and this ansatz reduces to the standard Hartree-Fock state. On the other hand, if the parent Hartree-Fock state breaks particle-hole symmetry, it can be verified that the two members of the pair are orthogonal to each other due to the Anderson orthogonality catastrophe. Again, the variational energy of the Slater pair does not improve with respect to standard mean-field theory. Thus, the long-range potential and hybridization in the parent Hamiltonian Eq. (13) are crucial to capture Kondo correlations. While more general Gaussian states [13,16,33,34] have been used recently, one of our main goals is to show that restricting parametrization to a site-dependent potential and hybridization suffices to obtain accurate results for the IRLM.

Above we presented an intuitive picture applicable when particle-hole conjugation symmetry is present. If an on-site energy is added to the impurity site, it cuts off Kondo physics at an energy scale equal to this bias. From a many-body perspective, the resulting ground state is less correlated than the unbiased case. It may, however, require twice the number of variational parameters to capture because the Slater determinants in the ansatz no longer come in pairs that are exactly conjugate (see Ref. [11] for an illustration in the case of the spin-boson model).

C. Other approaches

To evaluate the quality of our trial state, it is useful to compare to existing methods based on comparable strategies. The most general of these is the one of Ashida *et al.*, which uses a canonical transformation to decouple the impurity from the bath [33,34]. The ground state of the transformed system is then approximated as a single Gaussian state [44,45]. This approach does not aim to achieve arbitrary accuracy and only explores a restricted region of Hilbert space. Nonetheless, the error it makes for the ground-state energy of the Kondo model is less than 0.5% in a significant portion of the phase diagram. Another attractive feature is that it has proved extensible to the description of dynamics. We will refer to this method as the canonically transformed Gaussian (CTG) approach.

To benchmark our approach, we applied the CTG approach directly to the IRLM. The appropriate canonical transformation for the Hamiltonian Eq. (6) is

$$T = \frac{1}{\sqrt{2}}[1 + P(2n_{-1} - 1)], \tag{18}$$

with the particle-hole conjugation operator P defined in Eq. (10). This transforms the conserved charge-conjugation parity into the occupation index of the localized orbital, i.e., $TPT^\dagger = 1 - 2n_{-1}$. In the symmetric phase and in the untransformed frame, the unique ground state has charge conjugation parity -1. Hence, in the transformed frame, the localized orbital is occupied. In the ground-state sector where $n_{-1} = 1$, the transformed Hamiltonian for sites $n = 0, 1, \ldots, 2\Omega$ reads

$$THT^\dagger = \frac{U}{2}\left(n_0 - \frac{1}{2}\right) + \gamma c_0 \mathcal{P} + \sum_{n=0}^{2\Omega-1}(t_n c^\dagger_n c_{n+1} + \text{H.c.}), \tag{19}$$

where

$$\mathcal{P} = (c^\dagger_{2\Omega} + c_{2\Omega})(c^\dagger_{2\Omega-1} - c_{2\Omega-1})\ldots(c^\dagger_0 + c_0) \tag{20}$$

is the charge conjugation operator for the many-body system consisting of sites 0 to 2Ω such that $\mathcal{P}^\dagger = \mathcal{P}$, $\mathcal{P}^2 = 1$ and $\mathcal{P}c_n\mathcal{P} = (-1)^n c^\dagger_n$, $n = 0, 1, \ldots, 2\Omega$. Note that the transformed Hamiltonian is completely nonlocal due to the term $\gamma c_0 \mathcal{P}$. In the transformed frame, the exact ground state takes the form $c^\dagger_{-1}|\Psi\rangle$, where $|\Psi\rangle$ is the many-body ground state of Eq. (19). The CTG approach assumes a trial state $c^\dagger_{-1}|G\rangle$, in which the Gaussian state $|G\rangle$ is the ground state of a generic quadratic parent Hamiltonian,

$$H_G = \sum_{mn=0}^{2\Omega}(h_{mn}c^\dagger_m c_n + \Delta_{mn}c^\dagger_m c^\dagger_n + \Delta^*_{mn}c_n c_m), \tag{21}$$

with $n_{-1}|G\rangle = 0$. Mapping back to the original frame, the CTG ansatz for the ground state of H in Eq. (6) then reads

$$|\psi_{\text{CTG}}\rangle = \frac{1}{\sqrt{2}}(c^\dagger_{-1}|G\rangle - \mathcal{P}|G\rangle), \tag{22}$$

The CTG state is obtained by optimization over all possible parent Hamiltonians H_G.

Two well-known earlier variational schemes can be obtained from the trial state Eq. (22) by placing restrictions on the Gaussian state $|G\rangle$. When $|G\rangle$ is taken to be of the form

$$\sum_{m=0}^{2\Omega}\psi_m c^\dagger_m|F\rangle, \tag{23}$$

where $|F\rangle$ is the $(\Omega - 1)$-particle Fermi sea ground state of the Wilson chain Eq. (6) with $U = 0$, $\gamma = 0$, and $n_{-1} = 0$, one obtains the equivalent of Yosida's Kondo trial state [46], translated into the language of the IRLM. Alternatively, when

the parent Hamiltonian H_G is taken to be of the form

$$\sum_{n=0}^{2\Omega-1} t_n(c_n^\dagger c_{n+1} + c_{n+1}^\dagger c_n) + \sum_{n=0}^{2\Omega} v_n c_n^\dagger c_n, \tag{24}$$

i.e., the kinetic term of the Wilson chain, plus a particle-hole-symmetry breaking on-site energy v_n, one obtains the IRLM equivalent of the original Silbey-Harris [9,37] approximation for the Ohmic spin-boson model.

It is important to note that the CTG state does not contain terms of the form $c_{-1}^\dagger c_n$ or $c_n^\dagger c_{-1}$ that hybridize the localized orbital with the rest of the chain, while our parent Hamiltonians do include such terms. The omission of such terms in the CTG approach is a reasonable price to pay to have a formalism that applies to generic systems in which the impurity may have very different degrees of freedom from the bath. However, in situations where the combined impurity plus bath constitutes a system of indistinguishable particles, it seems reasonable to include hybridization terms. For the IRLM, the hybridization terms allow the ansatz to reduce to the exact ground state when $U = 0$, and to be at least as accurate as Hartree-Fock mean field theory when $U \neq 0$. On the other hand, the CTG parent Hamiltonian contains pairing terms $\Delta_{mn} c_m^\dagger c_n^\dagger + \Delta_{mn}^* c_n c_m$. This may capture many-body correlations beyond the reach of a single Slater determinant. It is interesting to ask whether or not these terms mimic the effect of hybridization terms in our approach. We also note that the number of variational parameters in the CTG approach scales quadratically with the system size, whereas in our approach it scales linearly.

III. NUMERICAL RESULTS

A. Ground-state energy

We now present numerical results in which we compare our Slater pair ansatz, optimized to yield the lowest possible variational energy E_{var}, to various results: Hartree Fock mean-field theory, the CTG approach, and NRG. In the absence of (numerically) exact methods, one can assess the accuracy of a variational trial state by calculating the standard deviation of the energy in the trial state, and comparing this to an estimate of the energy scale (such as the Kondo temperature) of the physics one hopes to capture. However, in the present case, the NRG results are very precise (nine or more significant digits), and we assess the accuracy of approximate trial states by comparing to NRG.

Unless otherwise stated, results are for the IRLM Wilson chain with $\Lambda = 1.5$, which allows good convergence to the thermodynamic limit of most observable quantities. We chose the size parameter $\Omega = 28$, which translates into a system of 29 particles distributed among 58 orbitals and an infrared cutoff scale of $10^{-5}t$. We fixed the hybridization to $\gamma = 0.15t$. If hybridization is increased, the ansatz becomes more accurate but the separation of scales between Kondo and ultraviolet physics, required for universality, eventually becomes lost. The considerations that dictated this choice of parameters are further explained in Appendix C. With the parameters as chosen here, the Kondo length becomes larger than the system size for $U < -0.9t$. We are thus able to probe fully developed Kondo correlations for interaction strengths $U > -0.9t$. Our goal is not only to show that the trial state yields a reasonable estimate for the ground-state energy but also that it accurately reproduces the correlation structure encoded in the covariance matrix Q. To do so, we will compare NRG and variational results for the spectrum of $Q(1-Q)$.

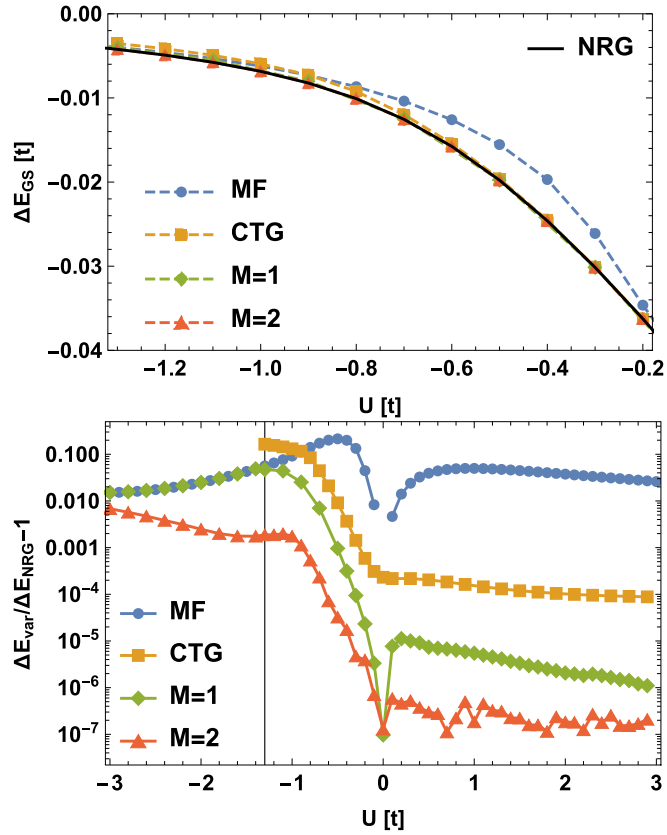

FIG. 1. Top panel: Relative ground state energy ΔE_{GS} of the IRLM measured with respect to the $\gamma = 0$ ground-state energy, as a function of interaction strength U. Results are for the Wilson chain with $\Omega = 28$ sites, discretization parameter $\Lambda = 1.5$, and hybridization $\gamma = 0.15t$. We compare the essentially exact NRG results to Hartree-Fock mean field theory (MF), the CTG approach, and the $M = 1$ and $M = 2$ Slater pair approximations. Bottom panel: Relative error $\Delta E_{\text{var}}/\Delta E_{\text{NRG}} - 1$ with respect to the NRG computation, shown in log scale and for a larger region of the U axis than in the top panel.

The first variational results we present are for the optimized energy E_{var} as a function of U. In Fig. 1, we compare the different variational approaches with NRG. Here are shown results for Hartree-Fock mean field theory, the CTG approach, and the $M = 1$ and $M = 2$ Slater pair approximations. For a given value of U, we compute the relative ground-state energy ΔE_{GS} with respect to the ground-state energy of the corresponding system with $\gamma = 0$. This subtracts a large kinetic energy contribution of the particles in the chain as well as a trivial contribution $\sim -|U|/4$ at large $|U|$. We denote energies measured from this offset as ΔE_{var} for the variational states and ΔE_{NRG} for the NRG benchmark. Both decrease monotonically as a function of U, from 0 at large negative U to $-|\gamma|$ at large positive U.

Comparing the Slater pair approximation to the numerically exact NRG calculation and Hartree-Fock, we see the following. In the phase with broken particle-hole symmetry ($U < -1.3t$), the $M = 1$ ansatz is equivalent to Hartree-Fock mean field theory, whereas in the symmetric phase it clearly outperforms the latter. Indeed Hartree-Fock predicts spontaneous symmetry breaking (nonzero value of $\langle n_{-1}\rangle - 1/2$) already for $U < -0.3t$. In the interval $-1.3t < U < 0$, the relative error associated with the $M = 1$ ansatz drops rapidly from 0.05 of the ground-state energy to zero. For $U = -0.9t$, where Kondo correlations become fully developed, the $M = 1$ ansatz produces a relative error of less than 1%. The $M = 1$ ansatz makes an error that is typically five times smaller than the CTG approach in the interval $-1.3t < U < 0$, while involving far fewer variational parameters. For positive U, the relative error is at most 10^{-5} of the ground-state energy, dropping to 10^{-6} at $U = 3t$. The error is between 20 and 100 times smaller than that associated with the CTG approach, showing that the Slater pair ansatz embodies a better representation of the physics of the IRLM ground state.

Improving our ansatz by using $M = 2$ Slater pairs further lowers the ground-state energy. In the symmetry-broken phase for $U = -2t$, the error is ten times smaller than Hartree Fock, and the absolute error is $4 \times 10^{-6}t$. At the phase transition, the relative error is 5×10^{-3} of the ground-state energy, or 20 times smaller than Hartree Fock. The relative error at $U = -0.9t$, where Kondo correlations are fully developed, is one part in 1000, two orders of magnitude more accurate than the CTG approach. For larger U, the error rapidly drops further. For $-0.9t < U < 0$, the $M = 2$ ansatz is typically between two and four orders of magnitude more accurate than Hartree-Fock, and two orders of magnitude more accurate than the CTG approach. For $U > 0$, the maximum relative error is 10^{-6} of the ground-state energy and drops to 10^{-7} at $U = 3t$. This is about three orders of magnitude more accurate than the CTG approach.

The interesting part of the IRLM's parameter space roughly corresponds to $-1.3\,t < U < 0$, where the Kondo temperature is significantly less than the ultraviolet scale t. To assess the accuracy of our approximation in this regime, one can compare the Kondo temperature to $E_{\rm var} - E_{\rm NRG}$. If $E_{\rm var} - E_{\rm NRG}$ is sufficiently smaller than T_K, the variational state accurately captures low-temperature Kondo correlations in the IRLM. We note that realistic Kondo temperatures are typically around 10^2 to 10^3 times smaller than the ultraviolet scale set by the band width (or Fermi energy). Now consider our results at $U = -0.8\,t$. Here the Kondo temperature is $\sim 10^{-4}\,t$, i.e., small by realistic standards. The true ground-state energy is $\sim -\,10^{-2}\,t$ and the error associated with the $M = 2$ ansatz is $3 \times 10^{-4}|E_0|$, i.e., it equals $3 \times 10^{-6}\,t$. Since this is 30 times less than the energy scale where Kondo physics sets in, the $M = 2$ ansatz describes Kondo physics very well for realistic couplings. For completeness, we replot $E_{\rm var} - E_{\rm NRG}$ in units of T_K in the interval $U \in [-1.0\,t, -01\,t]$ in Appendix D, for the CTG, $M = 1$, and $M = 2$ Slater pair approaches.

When M was increased beyond 2 (not shown), our rudimentary global minimization procedure yielded only very small improvements in the ground-state energy. In principle, it could be that for the IRLM, $O(N)$-parameter parent Hamiltonians are not sufficient to obtain arbitrary accuracy. However, we think it more likely that further significant convergence to the ground state can be obtained by increasing M beyond 2, if a more sophisticated minimization procedure is employed. We base this statement on results obtained for the ohmic spin-boson model, using trial states consisting of superpositions of coherent bath states entangled with the spin impurity [11,12]. Using bosonization identities, the trial state for the spin-boson model can be related to a superposition of Slater pairs for which parent Hamiltonians are endowed with a Hartree channel only. This leads to slower initial convergence as a function of M, but the simpler bosonic description revealed crucial analytical insights about the structure of the minimization problem that allowed for efficient minimization up to $M \sim 10$. Power-law convergence (without saturation) with increasing M was seen. We did not pursue the question of M convergence in the IRLM further because the $M = 2$ ansatz is already sufficiently accurate for realistic Kondo temperatures of order 10^4 times smaller than the Fermi energy. Yet, optimizing the convergence of the minimization algorithm for Slater pair states remains an important issue, as considered, for instance, in the recent Ref. [16].

Examining the CTG approach further, we find that there is no pairing in the region $U > -0.9t$ where Kondo correlations are fully developed. In other words, in this regime, $|G\rangle$ reduces to an Ω-particle Fermi sea (Slater determinant). Thus we conclude that pairing correlations allowed in the CTG approach are not able to mimic the hybridization terms included in the parent Hamiltonians of the Slater pair approximation. We stress that this conclusion is for the IRLM. Although the IRLM is equivalent to the Kondo model, applying the CTG approach to the Kondo model is in principle not equivalent to applying it to the IRLM. Since the fermions in the IRLM are squares of the fermions in the Kondo model, the degrees of freedom that are assigned a Gaussian correlation structure are not the same in the two cases. Nonetheless, in their application of the CTG approach to the Kondo model, Ashida *et al.* found similar relative errors as we did for the IRLM, ranging from around 0.1 close to the phase transition to $\sim 10^{-4}$ deep in the symmetric phase. We do not show CTG results for the symmetry-broken phase of the IRLM. In this phase, the restrictions placed on the CTG trial state conspire with the orthogonality catastrophe to produce a result that is guaranteed to be worse than Hartree-Fock mean-field theory. It should be noted that, in contrast, when the CTG approach is applied to the Kondo model, the ferromagnetic phase, equivalent to the symmetry-broken phase of the IRLM, yields the most accurate results, indicating that CTG performs better for the Kondo model than for the IRLM, presumably due to the fact that the Kondo impurity spin is distinguishable from the bath electronic states.

B. Covariance matrix spectrum

We have demonstrated that, unlike mean-field theory, or the CTG approach, the $M = 2$ Slater pair ansatz is reliable throughout the whole phase diagram of the IRLM and is nearly exact for $U > 0$. We now focus on the strongly correlated physics of the symmetric phase, $-0.9t < U < 0$, for the chosen parameters of the model. Our aim is to further quantify

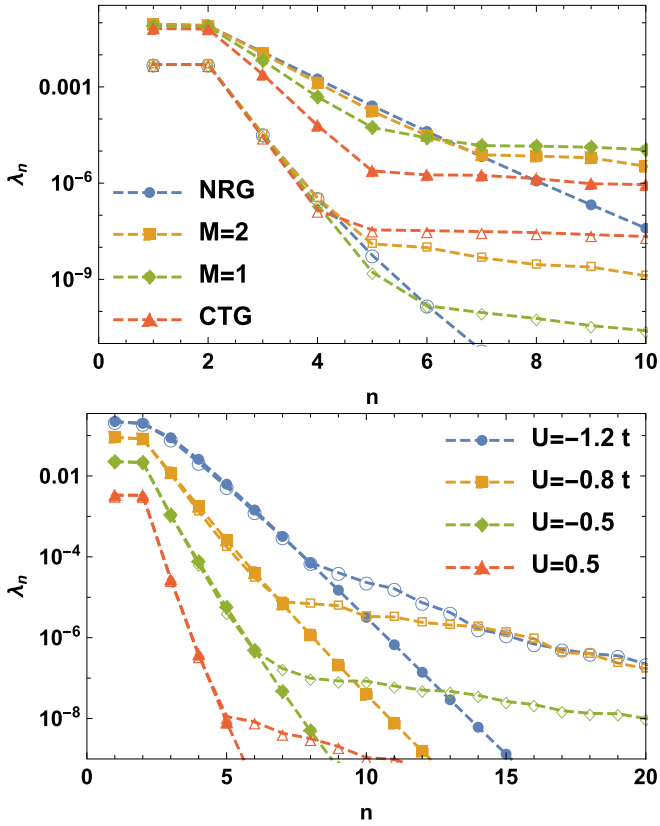

FIG. 2. Eigenvalue spectrum of $Q(1-Q)$. Top panel: Comparison between NRG, the CTG approach, and the $M=1$ and $M=2$ Slater pair approximations for $U=-0.6t$ (filled symbols) and $U=0.8t$ (open symbols). Results are for $\gamma=0.15t$, $\Lambda=1.5$, and $\Omega=28$. Bottom panel: Comparison between NRG and the $M=2$ Slater pair ansatz, at various U, for the same set of parameters.

the extent to which our variational approach reproduces the many-body correlations present in the ground state. For this purpose, we consider the covariance matrix Q Eq. (8). Before presenting results for our trial states, we review a few relevant properties of the Q spectrum. In the symmetric phase, particle-hole symmetry implies that the eigenvalues of $Q(1-Q)$ are at least twofold degenerate. When representing the correlation spectrum, we will show only one member of each pair and order them in decreasing order $\lambda_1 \geqslant \lambda_2 \geqslant \ldots \geqslant \lambda_{\Omega+1}$. NRG results reveal a further approximate twofold degeneracy of the largest eigenvalue of $Q(1-Q)$, i.e., $\lambda_1 \simeq \lambda_2$. Exponential decay abruptly sets in from λ_3, i.e., $\lambda_n = Ae^{-xn}$ for $n \geqslant 3$. The approximate fourfold degeneracy of the largest eigenvalues of $Q(1-Q)$ reveals a Bell-state-like nature of the IRLM ground state. This is related to the fact that at negative U, the localized orbital and site zero of the chain tend to be either both filled or both empty (similarly at positive U, if the localized orbital is filled, the site zero tends to be empty and vice versa).

In Fig. 2, we compare our variational results to NRG for the spectrum of $Q(1-Q)$. In the top panel, we present results for the CTG and $M=1$ and $M=2$ Slater pair approximations. We see that all three variational states produce good results for λ_1 and λ_2, the two largest eigenvalues that are most directly linked to the Bell-like nature of the particle-hole symmetric ground state. At $U=-0.8t$ (filled symbols), it is clear that eigenvalues λ_3 to λ_5 are underestimated more severely, the less accurate the variational state, i.e., the CTG approach gives the smallest eigenvalues, followed by $M=1$, and then $M=2$, which very nearly coincides with NRG. Recalling that all eigenvalues of $Q(1-Q)$ are zero for a single Slater determinant, the interpretation is as follows: The CTG approach and the $M=1$ ansatz underestimate eigenvalues λ_3 to λ_5 because these trial states are less correlated than the true ground state. We further see that beyond a certain index n, all variational states produce spurious plateaus in the spectra, whereas the true spectrum continues to decay exponentially with increasing n. These plateaus arise because a given family of variational states can only produce physical correlations above a certain resolution. Weaker correlations present in the variational state are determined not by physical effects but by the limited form imposed on the ansatz. For $U=-0.8t$, we see that the $M=2$ ansatz accurately reproduces λ_1 to λ_7, thus accounting for all eigenvalues down to 10^{-5}. At $U=0.8t$ (open symbols), all three trial states reproduce the spectrum of $Q(1-Q)$ well, down to eigenvalues $\sim 10^{-7}$. This is consistent with the increased accuracy of the ground-state energy at positive U with respect to negative U, as seen in Fig. 1. Not only do the eigenvalues decay faster for positive U, but their magnitude is also smaller for positive U than for negative U. Thus, the improved accuracy of all the variational states for positive U is tied to the fact that many-body correlations are weaker in this parameter regime. In the lower panel of Fig. 2, we compare the $M=2$ ansatz (open symbols) to NRG at various values of U. At $U=-1.2t$, the first eight eigenvalues are accurately reproduced, representing a threshold between 10^{-4} and 10^{-5}. This threshold improves to 10^{-8} at $U=0.5t$. However, at $U=0.5t$ the ground state contains weaker many-body correlations than close to the phase transition and, as a result, there are only five eigenvalues above the threshold to the spurious plateau behavior.

If the eigenvectors of Q, associated with eigenvalues significantly different to zero or one are known to good accuracy, an accurate approximation to the ground state can be constructed by solving a few-body problem in the Fock space built from only these orbitals [13,42]. The size of this few-body problem is independent of N, the actual system size. It is purely determined by the desired accuracy and the exponential decay rate of the spectrum of Q. It is therefore worth checking how accurately the Slater pair ansatz reproduces these eigenvectors. In Fig. 3, we compare eigenvectors associated with λ_1 and λ_6 at $U=-0.8t$, calculated with the Slater-pair ansatz, to NRG results. (This corresponds to one of the spectra shown in Fig. 2.) We see very good agreement.

It is interesting to note that the Slater pair ansatz remains accurate beyond the range of Λ accessible through NRG. Using NRG, we have verified that the spectrum of $Q(1-Q)$ has no discernible Λ dependence for $2 > \Lambda > 1.5$ [42]. This provides strong evidence that $\Lambda=1.5$ results have converged to the continuum limit Eq. (2). However, it is challenging to push the NRG calculation of Q well beyond $\Lambda=1.5$. In contrast to this, we could perform $M=2$ variational calculations at $U=-0.5\,t$, $\gamma=0.15\,t$, $\Omega=28$, and successively lower Λ. Results are presented in Fig. 4. We see that the part of the $Q(1-Q)$ spectrum that is accurately reproduced by the ansatz is insensitive to Λ, for $\Lambda \geqslant 1.2$, but changes

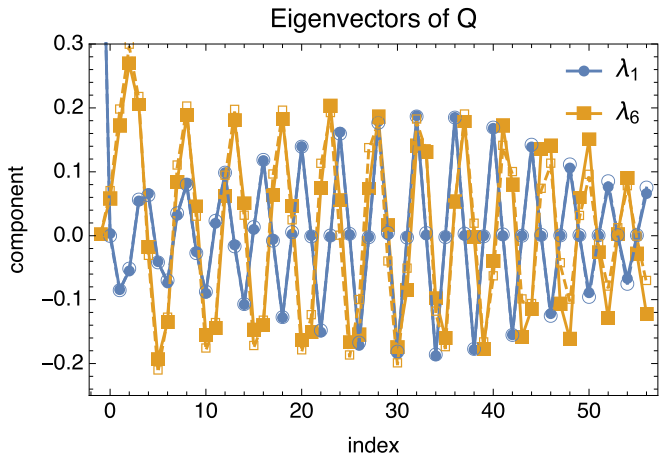

FIG. 3. Eigenvectors of Q associated with λ_1 and λ_6 in Fig. 2 at $U = -0.8t$. Closed symbols correspond to data calculated using the $M = 2$ ansatz, while open symbols represent NRG results.

significantly for $\Lambda = 1.1$. To understand this, we note that the Kondo temperature $T_K \sim 3 \times 10^{-3} t$ is of the same order as the infrared cutoff for $\Lambda = 1.2$, and an order of magnitude smaller than the infrared cutoff when $\Lambda = 1.1$. (The number of sites on the Wilson chain was kept fixed when changing the Λ parameter.) We conclude that the spectrum of $Q(1-Q)$ is insensitive to Λ as long as the Kondo temperature is larger than the infrared cutoff. We therefore expect the spectrum of $Q(1-Q)$ to remain invariant if we take the continuum limit by first sending the infrared cutoff to zero ($\Omega \to \infty$) before sending $\Lambda \to 1$. This confirms that the exponential decay of eigenvalues is not an artifact of the logarithmic discretization of the conduction band and is an intrinsic property of the quantum impurity problem [13,42].

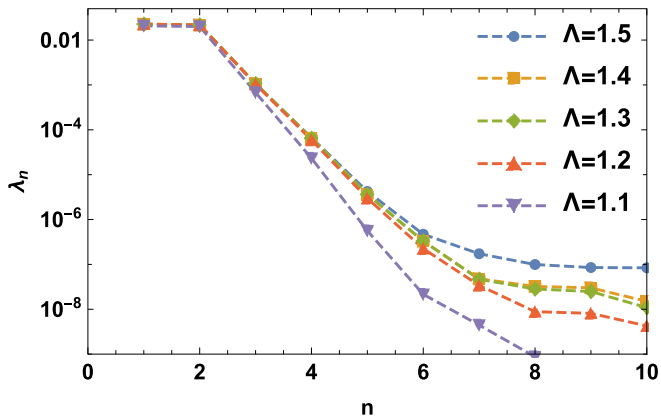

FIG. 4. Eigenvalue spectrum of $Q(1-Q)$ in descending order for various discretization parameters Λ, for $U = -0.5t$, $\gamma = 0.15t$, and $\Omega = 28$. Only one eigenvalue of each degenerate pair is plotted. Results were obtained variationally using $M = 2$ pairs of Slater determinants. The infrared scale $\Lambda^{-\Omega} t$ varies from $5 \times 10^{-6} t$ at $\Lambda = 1.5$ to $7 \times 10^{-2} t$ at $\Lambda = 1.1$, while the Kondo temperature is $3 \times 10^{-3} t$. The apparent weakening of correlations for $\Lambda = 1.1$ is thus due to finite-size effects that cut off the full development of the Kondo state.

IV. DISCUSSION AND CONCLUSIONS

Quantum impurity problems in which a localized orbital hosts electrons that interact with a conduction band play an important role in the field of strongly correlated electrons. Here we investigated the many-body wave function of the simplest, spinless case known as the IRLM, a system that also provides a window into the Kondo problem. We formulated a variational ansatz that provides an intuitive picture of this wave function based on the superposition of Slater determinants and that accurately describes the zero temperature limit. Our rational was to restore a discrete symmetry that is spuriously broken in mean-field theory by forming appropriate linear combinations of symmetry-broken mean-field states. The key insight is that this must be done in a way that avoids the orthogonality catastrophe between symmetry-broken terms by introducing some extra freedom with respect to the mean-field functional. Thus we arrived at a state that is a linear combination of nonorthogonal Slater determinants, each associated with a different static scatterer in place of the dynamic impurity. Much like mean-field theory, the natural variational parameters are the matrix elements of the associated single-particle Hamiltonians. Focusing on the Hartree and Fock channels, we endowed each parent Hamiltonian with a set of variational parameters whose size scales linearly with the size of the system. We were able to obtain quantitatively accurate results up to very large correlation (Kondo) lengths. We compared our method to existing variational approaches that construct correlated states using uncorrelated electronic states as building blocks. The comparison to the CTG approximation [33,34] showed that pairing-type correlations, allowed by generic Gaussian states, are not relevant for the physics of the IRLM. Clarifying for which families of impurity models such off-diagonal correlations play a major role would be physically insightful.

We find that our method is significantly more accurate than comparable methods that do not harness the full power of the superposition principle. Indeed, it has recently been shown that superpositions of Gaussian states can approximate the ground states of fermionic impurity systems to any desired accuracy using resources that scale quasipolynomially in 1/accuracy [13]. Our result demonstrates that physical insight into the specific problem under consideration can lead to practical algorithms employing the superposition principle, for which the number of variational parameters are O(system size). This may significantly simplify the optimization problem compared to existing algorithms that use a general parametrization of Gaussian states, involving O(system-size^2) variational parameters.

By studying the eigenvalues of the covariance matrix Q, we were also able to quantify the extent to which our trial state encodes many-body correlations correctly. Requiring the ansatz to reproduce the spectrum of $Q(1-Q)$ is a far more stringent and unbiased criterium than reproducing expectation values for a small set of observables, such as energy and the order parameter. Again, the conclusion is that our ansatz does an excellent job even at very large correlation lengths. As the critical interaction strength U_c is approached from within the symmetric phase, the ground state becomes more and more correlated. (The spectrum of Q has more and more

eigenvalues significantly different from zero or one.) It is interesting to note the significant improvement in accuracy that is obtained in this regime when a second Slater pair ($M = 2$) is added to the single pair ($M = 1$) ansatz. It implies that the introduction of new Slater pairs mirrors the buildup of correlations as the critical point is approached. We envision future work in which we develop numerical minimization methods that can efficiently explore the larger parameter space associated with more Slater pairs and in this way quantify the above statement more precisely. It would, for instance, be insightful to know how many Slater pairs are required for a specified accuracy, as a function of the distance from the critical point, and to relate it to the bound derived in Ref. [13].

We also envision future work in which the present method is extended to study nonequilibrium dynamics. As was done within the CTG approach, one could proceed by the standard method of projecting the dynamics onto the region of Hilbert space that is parametrized by the variational ansatz. The CTG ansatz is a restricted form of the superposed Gaussian ansatz. Thus, the same method, applied to Gaussian superpositions as considered in Ref. [13], is expected to be more accurate than the already successful CTG approach. It is then an open question whether our restriction to $O(N)$ variational parameters remains accurate for dynamical problems. We believe that the prospects are good, based on existing results for nonequilibrium dynamics of the ohmic spin-boson model [47,48]. Indeed, as we explained in Sec. I B, it can be seen via bosonization that the superposed Slater pair ansatz with its $O(N)$ parameters amounts to a generalization of the ansatz that was employed for the spin-boson model.

ACKNOWLEDGMENTS

We thank the National Research Foundation of South Africa (Grant No. 90657), and the CNRS PICS contract FERMICATS for support.

APPENDIX A: MATRIX ELEMENTS INVOLVING NON-ORTHOGONAL SLATER DETERMINANTS

To evaluate the matrix elements of the covariance matrix Q, and the expectation value of the Hamiltonian with respect to our trial state, we have to compute quantities of the form $\langle X|\hat{O}|Y\rangle$ where $\hat{O}$ is a product of up to four creation and annihilation operators from the set $\{c_m; c_m^\dagger | m = -1, 0, \ldots, 2\Omega\}$, while $|X\rangle$ and $|Y\rangle$ are single Slater determinants. What makes the situation slightly unusual is that the single-particle orbitals that are naturally associated with $|X\rangle$ and $|Y\rangle$ are drawn from distinct single particle bases, and hence the orbitals of $|X\rangle$ are not the same or orthogonal to those of $|Y\rangle$. In this Appendix, we derive simple formulas applicable to this situation. We start by defining the objects we need.

Let $N \leqslant 2\Omega + 2$ be the number of particles in the system. Let $\{x_\alpha|\alpha = 1, \ldots, N\}$ and $\{y_\alpha|\alpha = 1, \ldots, N\}$ be two sets of fermion annihilation operators. The members of each set can be expressed as linear combinations of $c_{-1}, \ldots, c_{2\Omega}$. We denote the respective expansion coefficients $X_{j\alpha}$ and $Y_{j\alpha}$, which are rectangular $(2\Omega + 2) \times N$ matrices. Throughout this Appendix, we will use Einstein summation convention to imply sums over repeated indices. We can thus write

$$x_\alpha^\dagger = c_j^\dagger X_{j\alpha},\ y_\alpha^\dagger = c_j^\dagger Y_{j\alpha}. \tag{A1}$$

Throughout, greek indices imply a range $\{1; \ldots; N\}$ over particles, while lowercase roman indices imply a range $\{-1; \ldots; 2\Omega\}$ over orbitals. Note that in contrast to the original fermions c_m, neither the x_α nor the y_α operators are associated with complete single-particle bases. In what follows below, we do not even need to assume that the orbitals associated with $\{x_\alpha|\alpha = 1, \ldots, N\}$ are mutually orthogonal, only that they are linearly independent. (The same goes for $\{y_\alpha|\alpha = 1, \ldots, N\}$.) We assume that the x_α and y_α operators are members of a different single-particle basis, so

$$\{x_\alpha, y_\beta^\dagger\} = M_{\alpha\beta},\ M = X^\dagger Y. \tag{A2}$$

Using our two sets of N creation operators, we construct two single-Slater determinants

$$|X\rangle = x_N^\dagger \ldots x_1^\dagger|0\rangle, \quad |Y\rangle = y_N^\dagger \ldots y_1^\dagger|0\rangle. \tag{A3}$$

The overlap between $|X\rangle$ and $|Y\rangle$ is therefore

$$\langle X|Y\rangle = \mathrm{Det}\, M. \tag{A4}$$

In the formulas we present below, we assume $\mathrm{Det}\, M \neq 0$, so M^{-1} exists. However, the limit $\mathrm{Det}\, M \to 0$ is regular.

First, we consider an arbitrary single-particle additive operator:

$$\hat{Z} = Z_{mn} c_m^\dagger c_n. \tag{A5}$$

We will prove that its overlap between two distinct Slater determinants can be evaluated as

$$\langle X|\hat{Z}|Y\rangle = \langle X|Y\rangle \mathrm{Tr}[X^\dagger Z Y M^{-1}]. \tag{A6}$$

For the purpose of the proof, we define new fermion creation operators, and an associated Slater determinant:

$$\bar{y}_\alpha^\dagger(\lambda) = e^{\lambda\hat{Z}} y_\alpha^\dagger e^{-\lambda\hat{Z}} = c_j^\dagger [e^{\lambda Z} Y]_{j\alpha},\ |\bar{Y}(\lambda)\rangle = e^{\lambda\hat{Z}}|Y\rangle. \tag{A7}$$

The anticommutator between x_α and $\bar{y}_\beta^\dagger(\lambda)$ evaluates to

$$\{x_\alpha, \bar{y}_\beta^\dagger(\lambda)\} = \bar{M}(\lambda)_{\alpha\beta}, \quad \bar{M}(\lambda) = X^\dagger e^{\lambda Z} Y, \tag{A8}$$

and the overlap between $|X\rangle$ and $|\bar{Y}(\lambda)\rangle$ gives

$$\langle X|\bar{Y}(\lambda)\rangle = \mathrm{Det}\, \bar{M}(\lambda). \tag{A9}$$

The result we want to prove now follows by noting that $\langle X|\bar{Y}(\lambda)\rangle$ can be used as a generating function for $\langle X|\hat{Z}|Y\rangle$, i.e.,

$$\begin{aligned}\langle X|\hat{Z}|Y\rangle &= \partial_\lambda \langle X|\bar{Y}(\lambda)\rangle|_{\lambda=0} \\ &= \partial_\lambda \exp \mathrm{Tr}\, \ln \bar{M}(\lambda)|_{\lambda=0} \\ &= \mathrm{Det}\, \bar{M}(\lambda) \mathrm{Tr}\, \{[\partial_\lambda \bar{M}(\lambda)]\bar{M}(\lambda)^{-1}\}\big|_{\lambda=0} \\ &= \langle X|Y\rangle \mathrm{Tr}[X^\dagger Z Y M^{-1}],\end{aligned} \tag{A10}$$

which completes the proof.

To compute the expectation value of interaction terms, we also need to evaluate quantities of the form $\langle X|\hat{Z}_1\hat{Z}_2|Y\rangle$ where both $\hat{Z}_1$ and $\hat{Z}_2$ are single-particle additive operators of the form Eq. (A5). We do so employing a strategy that is similar to the above. We use a generation function

$$\langle X|e^{\lambda_1\hat{Z}_1} e^{\lambda_2\hat{Z}_2}|Y\rangle = \mathrm{Det}(X^\dagger e^{\lambda_1 Z_1} e^{\lambda_2 Z_2} Y), \tag{A11}$$

such that

$$\langle X|\hat{Z}_1\hat{Z}_2|Y\rangle = \partial_{\lambda_2}\partial_{\lambda_1}\langle X|e^{\lambda_1\hat{Z}_1}e^{\lambda_2\hat{Z}_2}|Y\rangle|_{\lambda_1=\lambda_2=0}. \quad \text{(A12)}$$

On the right-hand side, we first take the λ_1 derivative and subsequently set λ_1 to zero to obtain

$$\partial_{\lambda_1}\langle X|e^{\lambda_1\hat{Z}_1}e^{\lambda_2\hat{Z}_2}|Y\rangle|_{\lambda_1=0} = \langle X|e^{\lambda_2\hat{Z}_2}|Y\rangle \mathrm{Tr}[X^\dagger Z_1 e^{\lambda_2 Z_2} Y (X^\dagger e^{\lambda_2 Z_2} Y)^{-1}]. \quad \text{(A13)}$$

Then taking the λ_2 derivative and setting λ_2 to zero, we arrive at the final result:

$$\langle X|\hat{Z}_1\hat{Z}_2|Y\rangle = \langle X|\hat{Z}_1|Y\rangle\langle X|\hat{Z}_2|Y\rangle/\langle X|Y\rangle + \langle X|Y\rangle \mathrm{Tr}[X^\dagger Z_1(1 - YM^{-1}X^\dagger)Z_2 Y M^{-1}]. \quad \text{(A14)}$$

While the above form will be most useful for our numerical calculations, further insight into the result can be gained by defining four new fermion annihilation operators $q_1, \ldots, q_4$, and two single-particle additive operators $q_1^\dagger q_2$ and $q_3^\dagger q_4$, i.e.,

$$q_i = c_j A_{ji}, \quad \hat{Z}_1 = q_1^\dagger q_2, \ \hat{Z}_2 = q_3^\dagger q_4. \quad \text{(A15)}$$

Substituting this $\hat{Z}_1$ and $\hat{Z}_2$ into the result Eq. (A14) and commuting q_2 past $q_3^\dagger q_4$, we obtain

$$\langle X|q_1^\dagger q_2^\dagger q_4 q_3|Y\rangle = \frac{1}{\langle X|Y\rangle}[\langle X|q_1^\dagger q_3|Y\rangle\langle X|q_2^\dagger q_4|Y\rangle - \langle X|q_1^\dagger q_4|Y\rangle\langle X|q_2^\dagger q_3|Y\rangle], \quad \text{(A16)}$$

which is a very straightforward generalization [49] of the familiar Wick's theorem when $|X\rangle = |Y\rangle$.

APPENDIX B: VARIATION OF THE ENERGY

We used a quasi-Newton method to optimize trial states. We thus had to calculate the expectation value

$$\langle E\rangle = \frac{\langle\psi|H|\psi\rangle}{\langle\psi|\psi\rangle} \quad \text{(B1)}$$

of the Hamiltonian with respect to the trial state, as well as its variation $\delta\langle E\rangle$ in response to changes of the variational parameters $\{f_J, \varepsilon_n^{(J)}, g_n^{(J)}\}$ appearing in the set of parent Hamiltonians Eq. (13). The expectation value $\langle E\rangle$ as well as its f_F derivatives can be calculated directly from the results of the previous section. The derivatives with respect to $\varepsilon_n^{(J)}$ and $g_n^{(J)}$ requires some further analysis, which we present here.

Let δ stand for the partial derivative with respect to any of the $\varepsilon_n^{(J)}$ or $g_n^{(J)}$. Note that the IRLM Hamiltonian as well as the parent Hamiltonians associated with our trial state can be simultaneously represented as real symmetric matrices. We can therefore perform our analysis in a real rather than complex Hilbert space, and this allows us to write the variation of $\langle E\rangle$ as

$$\delta\langle E\rangle = 2\frac{\langle\delta\psi|H|\psi\rangle - \langle E\rangle\langle\delta\psi|\psi\rangle}{\langle\psi|\psi\rangle}. \quad \text{(B2)}$$

Recall that our trial state is

$$|\psi\rangle = \sum_{J=1}^{M} f_J(1-P)|F_J\rangle, \quad \text{(B3)}$$

where $|F_J\rangle$ is the Fermi-sea ground state of the parent Hamiltonian H_J, and P the conjugation operator over all fermions. The partial derivative of the trial state is therefore related to the partial derivative δH_J of the parent Hamiltonian by first-order perturbation theory on H_J. We note that δH_J is a single-particle additive operator that creates one particle-hole pair in the Fermi sea $|F_J\rangle$. We denote by x_m $(m = 1, \ldots, 2\Omega+2)$ the fermion annihilation operators associated with the complete single-particle basis in which the given H_J that we are varying is diagonal. When referring to operators associated with the $\Omega+1$ lowest energy orbitals of H_J that are occupied, we use an unprimed greek index, i.e., x_α, $\alpha = 1, \ldots, \Omega+1$. When referring to one of the $\Omega+1$ highest energy orbitals of H_J, that are unoccupied, we use a primed greek index, i.e., $x_{\alpha'}$, $\alpha' = \Omega+2, \ldots, 2\Omega$. With these conventions, we then have

$$|\delta\psi\rangle = f_J \sum_{\alpha=1}^{\Omega+1}\sum_{\beta'=\Omega+2}^{2\Omega} x_{\beta'}^\dagger x_\alpha |F_J\rangle \Delta_{\alpha\beta'},$$
$$\Delta_{\alpha\beta'} = \frac{\langle F_J|x_\alpha^\dagger x_{\beta'}\delta H_J|F_J\rangle}{\varepsilon_\alpha^{(J)} - \varepsilon_{\beta'}^{(J)}}, \quad \text{(B4)}$$

and hence

$$\delta\langle E\rangle = 4 f_J \sum_{J'=1}^{M}\sum_{\alpha=1}^{\Omega+1}\sum_{\beta'=\Omega+2}^{2\Omega} \Delta_{\alpha\beta'} a_{J'} O_{J'\alpha\beta'},$$
$$O_{J'\alpha\beta'} = \frac{\langle F_J|x_\alpha^\dagger x_{\beta'} H|F_{J'}\rangle - \langle F_J|x_\alpha^\dagger x_{\beta'}(H - \langle E\rangle)|\tilde{F}_{J'}\rangle}{\langle\psi|\psi\rangle}, \quad \text{(B5)}$$

where we use the shorthand

$$|\tilde{F}_J\rangle = P|F_J\rangle \quad \text{(B6)}$$

for the particle-hole conjugate Slater determinant to $|F_J\rangle$.

By setting $|X\rangle = |F_J\rangle$ and either $|Y\rangle = |F_J\rangle$ or $|Y\rangle = |\tilde{F}_J\rangle$, we are left with the task of calculating $\langle X|x_\alpha^\dagger x_{\beta'} H|Y\rangle$. We focus on the term in H containing the density-density interaction between sites -1 and 0. The remaining terms in the Hamiltonian can be done using the same principles, but are simpler because they are single-particle additive terms.

We note that $x_{\beta'}^\dagger x_\alpha|X\rangle$ is a single Slater determinant. We can therefore apply Eq. (A16) and obtain

$$\langle X|x_\alpha^\dagger x_{\beta'} n_{-1} n_0|Y\rangle = \frac{\langle X|x_\alpha^\dagger x_{\beta'} n_{-1}|Y\rangle\langle X|x_\alpha^\dagger x_{\beta'} n_0|Y\rangle}{\langle X|x_\alpha^\dagger x_{\beta'}|Y\rangle} - \frac{\langle X|x_\alpha^\dagger x_{\beta'} c_{-1}^\dagger c_0|Y\rangle\langle X|x_\alpha^\dagger x_{\beta'} c_0^\dagger c_{-1}|Y\rangle}{\langle X|x_\alpha^\dagger x_{\beta'}|Y\rangle}. \quad \text{(B7)}$$

The expansion coefficients of x_m in terms of the c_m basis form a $(2\Omega+2)\times(2\Omega+2)$ real orthogonal matrix that we denote X', such that

$$x_m^\dagger = \sum_{j=-1}^{2\Omega} c_j^\dagger X'_{jm}. \quad \text{(B8)}$$

The rectangular $(2\Omega+2)\times(\Omega+1)$ subblock of X' corresponding to its first $\Omega+1$ columns corresponds to the matrix

X defined in the previous Appendix, i.e.,

$$X_{j\alpha} = X'_{j\alpha}. \tag{B9}$$

Setting $\hat{Z} = x^\dagger_\alpha x_{\beta'} = \sum_{jk=-1}^{2\Omega} X_{j\alpha} X'_{k\beta'} c^\dagger_j c_k$ and using Eq. (A6) along with the fact that $\sum_{j=-1}^{2\Omega} X_{j\nu} X_{j\alpha} = \delta_{\alpha\nu}$, we find that

$$\langle X | x^\dagger_\alpha x_{\beta'} | Y \rangle = \langle X | Y \rangle [(X')^\dagger Y M^{-1}]_{\beta'\alpha}. \tag{B10}$$

By further setting $\hat{Z}_2 = c^\dagger_j c_k$ in Eq. (A14), we find

$$\begin{aligned}&\langle X | x^\dagger_\alpha x_{\beta'} c^\dagger_j c_k | Y \rangle \\ &= \frac{\langle X | x^\dagger_\alpha x_{\beta'} | Y \rangle \langle X | c^\dagger_j c_k | Y \rangle}{\langle X | Y \rangle} \\ &\quad + \langle X | Y \rangle [(X')^\dagger (1 - Y M^{-1} X^\dagger)]_{\beta' j} [Y M^{-1}]_{k\alpha}. \end{aligned} \tag{B11}$$

When this is substituted back into Eq. (B7), one obtains a formula for $\langle X | x^\dagger_\alpha x_{\beta'} n_{-1} n_0 | Y \rangle$ that can be evaluated if X' is known. (Both Y and M^{-1} can be calculated if the X' of each term J is known.) We obtain X' by diagonalizing H_J numerically in the single-particle sector.

APPENDIX C: CHOICE OF PARAMETERS FOR THE NUMERICS

The following considerations informed our choice of parameters γ and Ω. There should be a reasonable separation of scales between the hybridization γ and bandwidth $2t$, otherwise universal many-body effects are obscured by nonuniversal ultraviolet effects. At the same time, if γ is too small, features in the energy landscape that are associated with important many-body physics become very shallow. Our relatively unsophisticated minimization procedure can easily miss such features. We find that $\gamma = 0.15t$ strikes a good compromise. Because we want to be reasonably sure of coming close to the absolute minimum of the energy landscape, we also avoid extremely long Wilson chains associated to exponentially small energy scales. We nonetheless want to have a system that is large enough to host fully developed Kondo correlations in a significant portion of the symmetric phase. We use $\Omega = 28$, which translates into a system with 29 particles distributed among 58 orbitals, and an infrared cutoff of $10^{-5}t$. Exploring the $E_{\text{var}}(\{f_J\}, \{\varepsilon^{(J)}_n\}, \{g^{(J)}_n\})$ landscape, we find (not unexpectedly) that there are spurious local minima. However, we also observe that it is not necessary to find the absolute minimum: there are many nearly degenerate minima that all give a very reasonable approximation to the true ground state. The proliferation of minima is most apparent in the $U > 0$ part of parameter space where the ansatz comes closest to the true ground state. Typical energy differences between minima are about an order of magnitude larger than the infrared cutoff $\sim 10^{-8}$. The various minima are likely associated with a few low-energy quasiparticles on top of the true ground state. To get a reasonable sampling of the energy landscape, we do 125 runs of a quasi-Newton (i.e., local) algorithm with randomized starting points and take the overall lowest found minimum. An evaluation of the energy or its gradient with respect to the variational parameters has a computational cost $\sim M^2 N^3$. The overall computational cost then depends on the details of the minimization algorithm. For our calculation, which is based on a fixed number of local minimization runs, the overall cost still scales like $\sim M^2 N^3$, but this does not guarantee reaching a predetermined accuracy. Our strategy works well for chains of length up to ~ 60 sites, and $M = 2$ Slater pairs. If one wanted to access longer chains (lower energies) or higher accuracy (more pairs), it seems one would need to adopt a more sophisticated global minimization strategy.

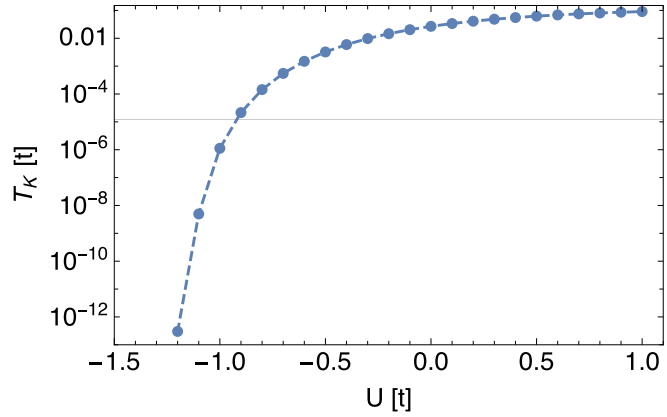

FIG. 5. Kondo temperature of the IRLM Wilson chain, versus U, calculated using NRG. $\gamma = 0.15\,t$, $\Lambda = 1.5$.

For $\Lambda = 1.5$ and $\gamma = 0.15t$, we need to know at which value of U the quantum phase transition occurs. We also need to know at what value of U in the symmetric phase that the emergent energy scale T_K becomes smaller than the infrared cutoff $10^{-5}t$. For this purpose, we performed NRG on a very long chain, and calculated T_K according to Eq. (4). Results are shown in Fig. 5. A horizontal line indicates the infrared cutoff associated with $\Omega = 28$. We see that the phase transition (where T_K vanishes) occurs close to $U = -1.3t$, and that T_K equals the infrared scale at around $U = -0.9t$. All further results presented in the main text are for $\Omega = 28$. We can expect to see fully developed strong correlations in the symmetric phase for $U \gtrsim -0.9t$. For $-1.3t < U < -0.9t$, the correlations associated with Kondo physics are only partially developed.

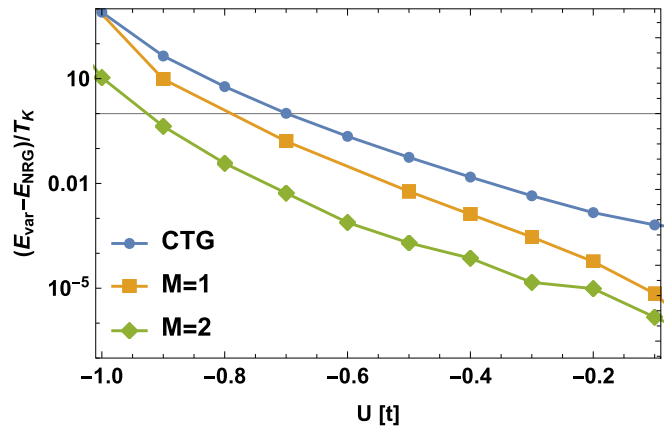

FIG. 6. $E_{\text{var}} - E_{\text{NRG}}$ in units of T_K versus U for the CTG, $M = 1$, and $M = 2$ Slater pair approaches, in the regime of universal Kondo correlations.

APPENDIX D: ACCURACY OF GROUND-STATE ENERGY COMPARED TO KONDO TEMPERATURE

As explained in Sec. III, it is instructive to compare the ground-state error $E_{\text{var}} - E_{\text{NRG}}$ to the Kondo temperature T_K, in the regime $-1.3\,t < U < 0$, where the Kondo temperature is significantly less than the ultraviolet scale, and the ground state hosts universal Kondo correlations. These correlations are captured by the variational state if the ground state error is less than the Kondo temperature. To judge the success of the various ansatze considered in this paper in the universal Kondo regime, we therefore plot the ground-state error in units of Kondo temperature in Fig. 6. As discussed in the main text, we see that at $U = -0.8\,t$, where the Kondo temperature is $1.4 \times 10^{-4}\,t$, the $M = 2$ ansatz achieves an error equal to a few percent of T_K. At this point, the CTG approach yields an error that is a hundred times bigger than T_K. The CTG approach eventually reaches an error in the few percent of T_K range, at $U = -0.4\,t$, where $T_K = 6 \times 10^{-3}\,t$.

[1] R. Bulla, T. A. Costi, and T. Pruschke, Numerical renormalization group method for quantum impurity systems, Rev. Mod. Phys. **80**, 395 (2008).

[2] S. R. White, Density Matrix Formulation for Quantum Renormalization Groups, Phys. Rev. Lett. **69**, 2863 (1992).

[3] U. Schollwöck, The density-matrix renormalization group in the age of matrix product states, Ann. Phys. **326**, 96 (2011), January 2011 Special Issue.

[4] E. Gull, A. J. Millis, A. I. Lichtenstein, A. N. Rubtsov, M. Troyer, and P. Werner, Continuous-time Monte Carlo methods for quantum impurity models, Rev. Mod. Phys. **83**, 349 (2011).

[5] G. Barcza, K. Bauerbach, F. Eickhoff, F. B. Anders, F. Gebhard, and O. Legeza, Symmetric single-impurity Kondo model on a tight-binding chain: Comparison of analytical and numerical ground-state approaches, Phys. Rev. B **101**, 075132 (2020).

[6] M. Greiter, V. Schnells, and R. Thomale, Method to identify parent Hamiltonians for trial states, Phys. Rev. B **98**, 081113(R) (2018).

[7] P. W. Anderson, Ground state of a magnetic impurity in a metal, Phys. Rev. **164**, 352 (1967).

[8] V. J. Emery and A. Luther, Ground-State Properties in the Kondo Problem, Phys. Rev. Lett. **26**, 1547 (1971).

[9] R. Silbey and R. A. Harris, Variational calculation of the dynamics of a two level system interacting with a bath, J. Chem. Phys. **80**, 2615 (1984).

[10] S. Bera, S. Florens, H. U. Baranger, N. Roch, A. Nazir, and A. W. Chin, Stabilizing spin coherence through environmental entanglement in strongly dissipative quantum systems, Phys. Rev. B **89**, 121108(R) (2014).

[11] S. Bera, A. Nazir, A. W. Chin, H. U. Baranger, and S. Florens, Generalized multipolaron expansion for the spin-boson model: Environmental entanglement and the biased two-state system, Phys. Rev. B **90**, 075110 (2014).

[12] S. Florens and I. Snyman, Universal spatial correlations in the anisotropic Kondo screening cloud: Analytical insights and numerically exact results from a coherent state expansion, Phys. Rev. B **92**, 195106 (2015).

[13] S. Bravyi and D. Gosset, Complexity of quantum impurity problems, Commun. Math. Phys. **356**, 451 (2017).

[14] L. Borda, Kondo screening cloud in a one-dimensional wire: Numerical renormalization group study, Phys. Rev. B **75**, 041307(R) (2007).

[15] B. Lechtenberg and F. B. Anders, Spatial and temporal propagation of Kondo correlations, Phys. Rev. B **90**, 045117 (2014).

[16] S. Boutin and B. Bauer, Quantum impurity models using superpositions of fermionic gaussian states: Practical methods and applications, Phys. Rev. Res. **3**, 033188 (2021).

[17] P. B. Vigman and A. M. Finkel'shtein, Resonant-level model in the Kondo problem, Sov. Phys. JETP **48**, 102 (1978).

[18] E. Boulat and H. Saleur, Exact low-temperature results for transport properties of the interacting resonant level model, Phys. Rev. B **77**, 033409 (2008).

[19] L. Borda, A. Schiller, and A. Zawadowski, Applicability of bosonization and the Anderson-Yuval methods at the strong-coupling limit of quantum impurity problems, Phys. Rev. B **78**, 201301(R) (2008).

[20] A. Braun and P. Schmitteckert, Numerical evaluation of Green's functions based on the Chebyshev expansion, Phys. Rev. B **90**, 165112 (2014).

[21] G. Camacho, P. Schmitteckert, and S. T. Carr, Exact equilibrium results in the interacting resonant level model, Phys. Rev. B **99**, 085122 (2019).

[22] B. Doyon, New Method for Studying Steady States in Quantum Impurity Problems: The Interacting Resonant Level Model, Phys. Rev. Lett. **99**, 076806 (2007).

[23] E. Boulat, H. Saleur, and P. Schmitteckert, Twofold Advance in the Theoretical Understanding of Far-From-Equilibrium Properties of Interacting Nanostructures, Phys. Rev. Lett. **101**, 140601 (2008).

[24] L. Borda and A. Zawadowski, Perturbative treatment of the multichannel interacting resonant-level model in steady-state nonequilibrium, Phys. Rev. B **81**, 153303 (2010).

[25] C. Karrasch, M. Pletyukhov, L. Borda, and V. Meden, Functional renormalization group study of the interacting resonant level model in and out of equilibrium, Phys. Rev. B **81**, 125122 (2010).

[26] S. Andergassen, M. Pletyukhov, D. Schuricht, H. Schoeller, and L. Borda, Renormalization group analysis of the interacting resonant-level model at finite bias: Generic analytic study of static properties and quench dynamics, Phys. Rev. B **83**, 205103 (2011).

[27] D. M. Kennes and V. Meden, Interacting resonant-level model in nonequilibrium: Finite-temperature effects, Phys. Rev. B **87**, 075130 (2013).

[28] L. Freton and E. Boulat, Out-of-Equilibrium Properties and Nonlinear Effects for Interacting Quantum Impurity Systems in the Strong-Coupling Regime, Phys. Rev. Lett. **112**, 216802 (2014).

[29] Y. Vinkler-Aviv, A. Schiller, and F. B. Anders, From thermal equilibrium to nonequilibrium quench dynamics: A conserving approximation for the interacting resonant level, Phys. Rev. B **90**, 155110 (2014).

[30] F. Schwarz, I. Weymann, J. von Delft, and A. Weichselbaum, Nonequilibrium Steady-State Transport in Quantum Impurity

Models: A Thermofield and Quantum Quench Approach Using Matrix Product States, Phys. Rev. Lett. **121**, 137702 (2018).

[31] M. E. Sorantin, W. von der Linden, R. Lucrezi, and E. Arrigoni, Nonequilibrium Green's functions and their relation to the negative differential conductance in the interacting resonant level model, Phys. Rev. B **99**, 075139 (2019).

[32] K. Bidzhiev, G. Misguich, and H. Saleur, Out-of-equilibrium transport in the interacting resonant level model: Surprising relevance of the boundary sine-Gordon model, Phys. Rev. B **100**, 075157 (2019).

[33] Y. Ashida, T. Shi, M. C. Bañuls, J. I. Cirac, and E. Demler, Solving Quantum Impurity Problems in and Out of Equilibrium with the Variational Approach, Phys. Rev. Lett. **121**, 026805 (2018).

[34] Y. Ashida, T. Shi, M. C. Bañuls, J. I. Cirac, and E. Demler, Variational principle for quantum impurity systems in and out of equilibrium: Application to Kondo problems, Phys. Rev. B **98**, 024103 (2018).

[35] K. Ohtaka and Y. Tanabe, Theory of the soft-x-ray edge problem in simple metals: Historical survey and recent developments, Rev. Mod. Phys. **62**, 929 (1990).

[36] A. J. Leggett, S. Chakravarty, A. T. Dorsey, M. P. A. Fisher, A. Garg, and W. Zwerger, Dynamics of the dissipative two-state system, Rev. Mod. Phys. **59**, 1 (1987).

[37] R. A. Harris and R. Silbey, Variational calculation of the tunneling system interacting with a heat bath. II. Dynamics of an asymmetric tunneling system, J. Chem. Phys. **83**, 1069 (1985).

[38] F. Guinea, V. Hakim, and A. Muramatsu, Bosonization of a two-level system with dissipation, Phys. Rev. B **32**, 4410 (1985).

[39] G. Kotliar and Q. Si, Toulouse points and non-Fermi-liquid states in the mixed-valence regime of the generalized anderson model, Phys. Rev. B **53**, 12373 (1996).

[40] T. A. Costi and G. Zaránd, Thermodynamics of the dissipative two-state system: A Bethe-ansatz study, Phys. Rev. B **59**, 12398 (1999).

[41] M. T. Fishman and S. R. White, Compression of correlation matrices and an efficient method for forming matrix product states of fermionic Gaussian states, Phys. Rev. B **92**, 075132 (2015).

[42] M. Debertolis, S. Florens, and I. Snyman, Few-body nature of Kondo correlated ground states, Phys. Rev. B **103**, 235166 (2021).

[43] M. Hanl and A. Weichselbaum, Local susceptibility and Kondo scaling in the presence of finite bandwidth, Phys. Rev. B **89**, 075130 (2014).

[44] C. V. Kraus and J. I. Cirac, Generalized HartreeFock theory for interacting fermions in lattices: Numerical methods, New J. Phys. **12**, 113004 (2010).

[45] C. Weedbrook, S. Pirandola, R. García-Patrón, N. J. Cerf, T. C. Ralph, J. H. Shapiro, and S. Lloyd, Gaussian quantum information, Rev. Mod. Phys. **84**, 621 (2012).

[46] K. Yosida, Bound state due to the $s-d$ exchange interaction, Phys. Rev. **147**, 223 (1966).

[47] N. Gheeraert, S. Bera, and S. Florens, Spontaneous emission of Schrödinger cats in a waveguide at ultrastrong coupling, New J. Phys. **19**, 023036 (2017).

[48] N. Gheeraert, X. H. H. Zhang, T. Sépulcre, S. Bera, N. Roch, H. U. Baranger, and S. Florens, Particle production in ultrastrong-coupling waveguide qed, Phys. Rev. A **98**, 043816 (2018).

[49] P.-O. Löwdin, Quantum theory of many-particle systems. I. Physical interpretations by means of density matrices, natural spin-orbitals, and convergence problems in the method of configurational interaction, Phys. Rev. **97**, 1474 (1955).